

Direct Josephson coupling between superconducting flux qubits

M. Grajcar,^{1,2} A. Izmalkov,^{1,3} S.H.W. van der Ploeg,^{1,4} S. Linzen,¹ E. Il'ichev,^{1,*} Th. Wagner,¹ U. Hübner,¹ H.-G. Meyer,¹ Alec Maassen van den Brink,^{5,†} S. Uchaikin,^{5,1} and A.M. Zagoskin^{5,6,‡}

¹*Institute for Physical High Technology, P.O. Box 100239, D-07702 Jena, Germany*

²*Department of Solid State Physics, Comenius University, SK-84248 Bratislava, Slovakia*

³*Moscow Engineering Physics Institute (State University), Kashirskoe shosse 31, 115409 Moscow, Russia*

⁴*MESA+ Research Institute and Faculty of Science and Technology,*

University of Twente, P.O. Box 217, 7500 AE Enschede, The Netherlands

⁵*D-Wave Systems Inc., 320-1985 W. Broadway, Vancouver, V6J 4Y3 Canada*

⁶*Physics and Astronomy Dept., The University of British Columbia,
6224 Agricultural Rd., Vancouver, V6T 1Z1 Canada*

(Dated: September 14, 2018)

We have demonstrated strong antiferromagnetic coupling between two three-junction flux qubits based on a shared Josephson junction, and therefore not limited by the small inductances of the qubit loops. The coupling sign and magnitude were measured by coupling the system to a high-quality superconducting tank circuit. Design modifications allowing to continuously tune the coupling strength and/or make the coupling ferromagnetic are discussed.

PACS numbers: 74.50.+r, 85.25.Am, 85.25.Cp

Quantum superposition of macroscopic states was conclusively demonstrated in superconducting Josephson structures in 2000.¹ Such structures are natural candidates for the role of qubits (quantum bits), the constituent elements of quantum computers. Successful operation of a quantum computer would be the ultimate confirmation of the validity of quantum mechanics on the macroscopic scale, which makes the task of controllably linking a significant number of qubits together more than just an advance in technology.

The coupling energy J must be comparable to the splittings between the two lowest eigenstates of individual qubits. On the other hand, the coupling must not excite the qubits to higher levels, or significantly increase the qubits' interaction with undesirable degrees of freedom, leading to decoherence and dissipation. Finally, J should be either variable by design or, even better, tunable during the system's operation.

In this letter we demonstrate the coupling of two three-Josephson-junction (3JJ) flux qubits, making progress towards meeting these requirements, and discuss the ways of its further improvement. The 3JJ qubit consists of a superconducting loop with small inductance L interrupted by three Josephson junctions. The two different directions of persistent current in the loop form the qubit's basis states.² The 3JJ design enables classical bistability even for $L \rightarrow 0$, resulting in a weak coupling to environmental magnetic flux noises. As a result, quantum behaviour with long decoherence time was observed in this type of qubit by several groups.³⁻⁵

However, their small L makes it difficult to couple 3JJ qubits inductively; generally, J is smaller than the single-qubit level splitting. We therefore implement the proposals^{6,7} to directly link two qubits through a shared junction (Fig. 1). The resulting coupling not only is strong, but can also be varied independently of other design parameters by choosing the shared junction's size.

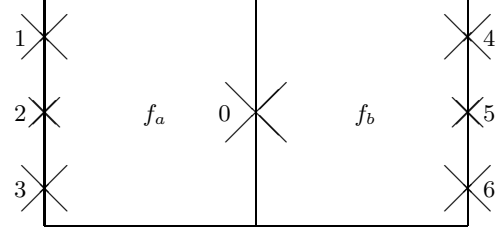


FIG. 1: Schematics of a 7JJ device: two 3JJ qubits with direct Josephson coupling and reduced flux bias $f_{a,b}$.

To calculate J , we neglect the inductances so that the potential term in the Hamiltonian contains only the Josephson energy $U_J = -\sum_{j=0}^6 E_j \cos \phi_j$, and use flux quantization, $\phi_1 + \phi_2 + \phi_3 + \phi_0 = 2\pi(\frac{1}{2} + f_a)$ and $\phi_4 + \phi_5 + \phi_6 - \phi_0 = 2\pi(\frac{1}{2} + f_b)$, to eliminate $\phi_{2,5}$ ($f_{a,b} = \Phi_{a,b}^x / \Phi_0 - \frac{1}{2}$ is the reduced flux bias). In the simplest case [$f_{a,b} = 0$; $E_{1,3,4,6} = E$; $E_{2,5} = \alpha E$ ($\frac{1}{2} < \alpha < 1$); $E_0 \gg E$] there are two different pairs of potential minima: “ferro-” and “antiferromagnetic” (with parallel and antiparallel loop currents respectively),

$$\begin{aligned} \phi_0^{\text{FM}} &= 0, \\ \phi_{1,3,4,6}^{\text{FM}} &= \pm \arccos(1/2\alpha); \end{aligned} \quad (1)$$

$$\begin{aligned} \phi_0^{\text{AF}} &= \pm \frac{\hbar I_p}{e E_0} + \mathcal{O}[(E/E_0)^2], \\ \phi_{1,3}^{\text{AF}} = -\phi_{4,6}^{\text{AF}} &= \pm \arccos(1/2\alpha) \pm \frac{1-2\alpha^2}{4\alpha^2-1} \frac{\hbar I_p}{e E_0} \\ &\quad + \mathcal{O}[(E/E_0)^2], \end{aligned} \quad (2)$$

where $I_p = (2e/\hbar)E\sqrt{1-1/4\alpha^2}$ is the persistent current in a free 3JJ qubit.² Inserting these into U_J , one finds

that the AF states have the lower energy by

$$\Delta U = 2J = \frac{\hbar^2 I_p^2}{2e^2 E_0} + \mathcal{O}[(E/E_0)^2], \quad (3)$$

so that the effective mutual inductance $\hbar^2/4e^2 E_0$ is just the standard Josephson inductance of the coupling junction.⁸ For an explanation, note that flipping the signs of $\phi_{4;6}^{\text{FM}}$ yields an AF configuration with $\phi_0 = 0$, and with the same energy as the FM minimum. Such a state of course is non-stationary (since charge must be conserved), and adjustment of the phases will lower U_J , with the stationary AF state (2) realizing the global minimum. More intuitively: the nonzero ϕ_0^{AF} reduces the effective frustration in the individual qubits, which is maximal for $f_{a;b} = 0$ [cf. above (1)]; the attendant reduction in qubit energy overcomes (by a factor two) the increase in Josephson energy in the coupling junction itself.

Thus the direct Josephson coupling of 3JJ qubits has the same sign as their inductive coupling (the latter corresponding to the natural north–south alignment of their magnetic moments),⁹ but is not restricted by the geometric inductances. For $E_0 \rightarrow \infty$, J in (3) disappears as it should, since then we have two qubits sharing a common leg without a junction—equivalent to two adjacent qubits if kinetic inductance is neglected, with only inductive coupling.¹⁰

We determined J using an impedance measurement technique, applied previously to 3JJ qubits^{4,11} and extended to multiple qubits in Ref. 12. The qubits are placed inside a tank circuit with known self-inductance L_T and quality factor Q_T , driven by a dc bias plus a small ac current at its resonance frequency ω_T (Fig. 2). The tank’s voltage–current phase angle θ is given by $\tan \theta = -(Q_T/L_T)\chi'$. Here, χ' is the qubits’ contribution to the tank susceptibility,¹³ readily related to the curvature of their energy bands: for qubit–tank mutual inductances $M_{aT} = M_{bT} \equiv M$, one has¹⁴

$$\tan \theta = \frac{Q_T}{L_T} M^2 \frac{d^2 E_{\text{tot}}}{d(\Phi^x)^2}, \quad (4)$$

where Φ^x denotes a symmetric change of flux bias in both qubit loops. At temperature $T = 0$, E_{tot} is the qubits’ ground-state energy; at finite T , the derivative simply becomes a Boltzmann average over the levels. The band curvature is large near anticrossings, so that $\tan \theta(f_a, f_b)$ contains important information about the level structure.

One obtains J from such a plot as follows. The standard four-state Hamiltonian for two coupled qubits is

$$H = -\epsilon_a \sigma_a^z - \Delta_a \sigma_a^x - \epsilon_b \sigma_b^z - \Delta_b \sigma_b^x + J \sigma_a^z \sigma_b^z, \quad (5)$$

where σ^x , σ^z are Pauli matrices, Δ_j is the tunneling amplitude, and $\epsilon_j = I_{pj} \Phi_0 f_j$ is the energy bias ($j = a, b$). For low T and small Δ_j , the *location* of the peaks in $|\tan \theta|$ (due to anticrossings) follows simply from the classical stability diagram. For instance, the $|\uparrow\downarrow\rangle \leftrightarrow |\uparrow\uparrow\rangle$ transition ($|\uparrow\downarrow\rangle: \sigma_a^z = -\sigma_b^z = 1$ etc.) occurs at $-\epsilon_a + \epsilon_b - J = -\epsilon_a - \epsilon_b + J \Rightarrow \epsilon_b = J$. Therefore, the peak-to-peak distance equals $2J$.

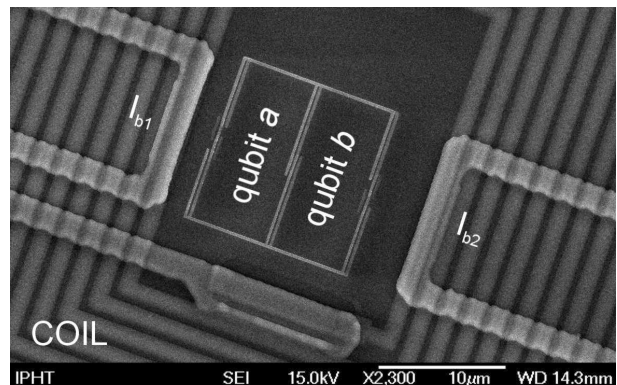


FIG. 2: Micrograph of sample 1 (see the table). The 3JJ qubits a and b are coupled through a shared Josephson junction, visible in the centre, and can be flux-biased independently by dc lines I_{b1} and I_{b2} . The pancake coil is part of an LC circuit reading out the qubits’ magnetic susceptibility.

For our samples, we first fabricate niobium (Nb) pancake coils and dc flux-bias lines on 4-inch oxidized silicon wafers, and then the qubits inside the coils by aluminium (Al) shadow evaporation on 12×12 mm² chips.

The Nb process starts with sputtering and dry etching of the 200 nm thick coil windings with 1 μm width, 1 μm line spacing, and typically 30 turns. The patterning uses e -beam lithography and a CF_4 RIE process. Then a silicon oxide isolation layer and the second 300 nm thick Nb film are deposited for the central coil electrode and the 2 μm wide dc lines; photolithography is used for all required resist masks of these layers. Finally, 400 nm silicon oxide is deposited for protection and isolation.

The Al process uses e -beam lithography to prepare the double layer resist mask for the qubits with a 150 nm linewidth. The two Al layers are deposited in situ by e -beam evaporation with different angles of incidence at a rate of 1.8 nm/s. The surface of the first Al film is oxidized with pure oxygen at a pressure of 10^{-2} mbar. The qubits are completed after the final lift-off.

Results are shown in Fig. 3(a). As explained below (5), one has $J \approx I_{pa} \Phi_0 \delta f_a = I_{pb} \Phi_0 \delta f_b$. One can find $I_{pa;b}$ in two different ways, which agree to within $\sim 20\%$. First, we used $I_p \approx I_c \sqrt{1 - 1/4\alpha^2}$ [cf. below (2)]. Here, I_c is the critical current of a junction fabricated on the same chip and with the same area of 650×150 nm² as junctions 1/3/4/6, enclosed in a superconducting loop and measured by the conventional rf-SQUID technique; $\alpha \approx 0.75$ by design. The second way is to fit the *shape* of the peaks in $\tan \theta(f_a, f_b)$ [Fig. 3(b)], using the spectrum of (5) to evaluate (4), which yields Δ_j and I_{pj} .^{11,12,15} The required tank parameters were extracted from its resonance characteristic, and the mutual inductances from the flux periodicity; for sample 1, $L_T = 136$ nH, $Q_T = 664$, $\omega_T/2\pi = 19.925$ MHz, and $M_{aT} = M_{bT} = 66.5$ pH. The $|\uparrow\downarrow\rangle \leftrightarrow |\downarrow\uparrow\rangle$ anticrossing does not show up in the figure because there is no net flux change, hence no contribution to the qubit susceptibility; one can also say that

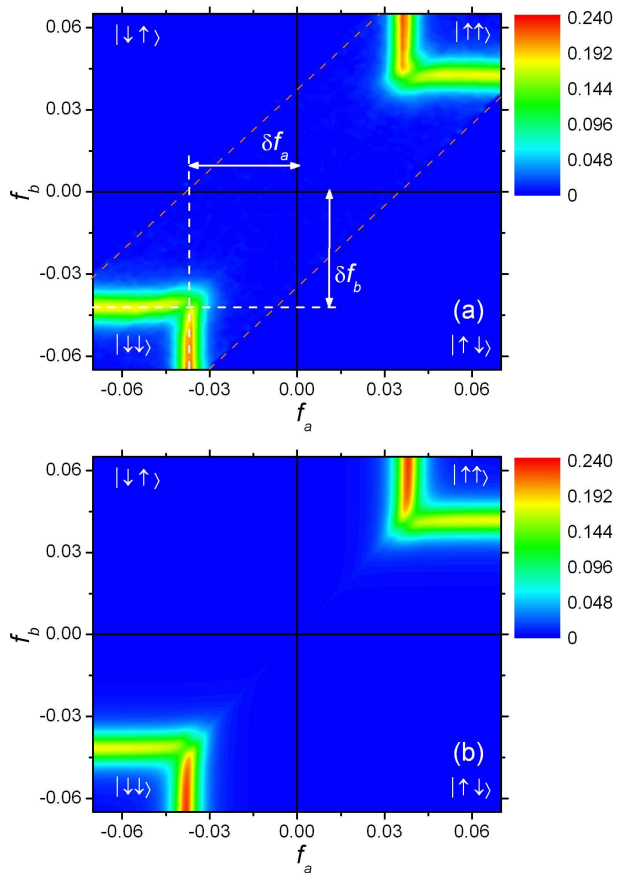


FIG. 3: Plot of $-\tan\theta(f_a, f_b)$ for two coupled 3JJ qubits (sample 1 from the table). (a): Measurements at a nominal mixing-chamber temperature of 20 mK (actual data taken between the dashed lines). (b): Theoretical fit for $T = 70$ mK (see the text for the different T 's). The coupling strength can be estimated from the separation between the peaks.

TABLE I: Coupling-junction areas S_0 , tunneling amplitudes Δ_j , persistent currents I_{pj} , coupling energies J , and peak locations δf for the measured samples.

sample No.	S_0 μm^2	Δ_a mK	Δ_b mK	I_{pa} nA	I_{pb} nA	J K	δf_{exp}	δf_{th}
1	0.30	80	90	120	110	0.7	0.037–0.041	0.0360
2	0.15	30	30	150	120	1.2	0.068	0.0675

the level curvature peaks perpendicular to the symmetric direction stipulated in (4).

The results of the fit are summarized in the table for two measured two-qubit samples, with different sizes of junction 0. Note how, say, $\Delta_a < \Delta_b$ for sample 1 makes the a -anticrossing sharper, resulting in a deeper colour for the corresponding peak (vertical bands in Fig. 3). Since $E_0/E = 3.1$ and 1.5 , respectively, the perturbative analysis leading to (3) does not apply quantitatively (the latter would have required large coupling junctions, which proved difficult to make with sufficient homogeneity). Instead, a theoretical prediction is made

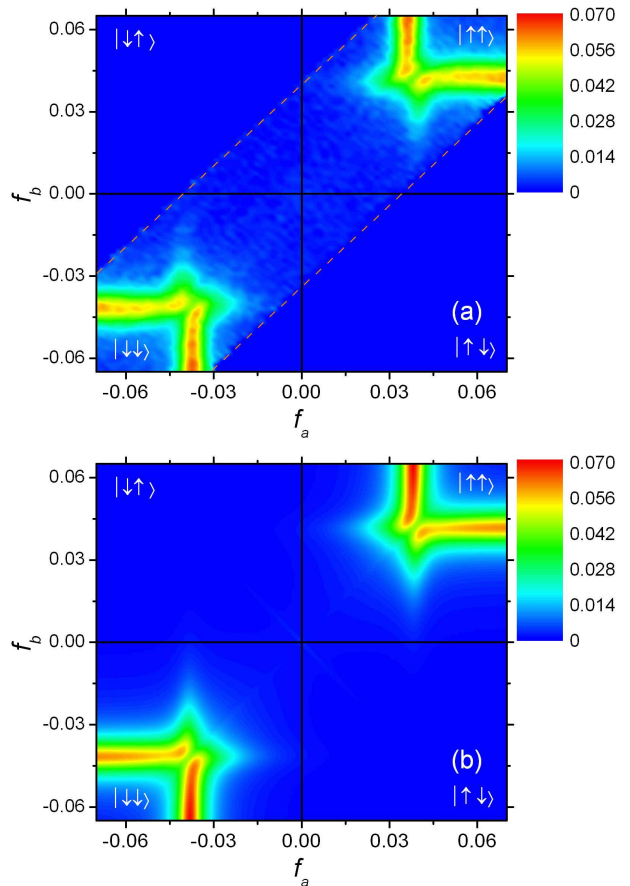


FIG. 4: As in Fig. 3, but for a mixing-chamber temperature of 200 mK (a) and an effective $T = 300$ mK (b).

for $\delta f(E_0/E, \alpha)$, by calculating the classical stability diagram directly from $U_J(\phi_0, \phi_1, \phi_3, \phi_4, \phi_6)$. Incidentally, this has the advantage that the critical-current density drops out of the comparison (last two columns in the table), which therefore shows greater accuracy than we can claim for J itself.

Data taken at a higher T support the effective Hamiltonian (5) for our 7JJ system beyond the ground state. Namely, for, say, $f_a \lesssim 0.035$, $f_b \approx 0.042$, an $|\downarrow\downarrow\rangle \leftrightarrow |\uparrow\uparrow\rangle$ anticrossing persists between excited states of sample 1. At finite T , it should contribute in (4), with rapidly decreasing Boltzmann weight as f_a is reduced. This is precisely what is seen in Fig. 4(a); the fit in Fig. 4(b) shows detailed agreement with the theory. In both Figs. 3 and 4, the discrepancy between effective and mixing-chamber temperatures is well within the range expected due to heating through external leads etc.; we observed no significant deviations from an equilibrium distribution.

The remarkable $J \sim 1$ K significantly exceeds both the tunnel splitting and the inductive coupling (estimated to be ~ 20 mK). It can be flux-tuned by using a standard compound junction (dc-SQUID) for the coupling. Instead, one can also apply a bias current I_b through junction 0.¹⁶ The corresponding generalization of (3) reads

$J = \hbar I_p^2 / 2e \sqrt{I_{c0}^2 - I_b^2} + \mathcal{O}[(E/E_0)^2]$. Thus, J can only be *increased*, albeit significantly. Hence, this mechanism does not allow, e.g., changing the coupling sign and tunable decoupling of qubits. These are desirable for most quantum algorithms, but existing proposals for flux qubits rely on, and therefore are limited by, mutual inductances.¹⁷ A bias line will introduce some noise. For reference, we give the coupling linewidth due to low-frequency fluctuations in I_b with spectral density $S_b(\omega)$: $\Delta J = \hbar I_p^4 I_b^2 S_b(0) / 4e^2 (I_{c0}^2 - I_b^2)^3$.

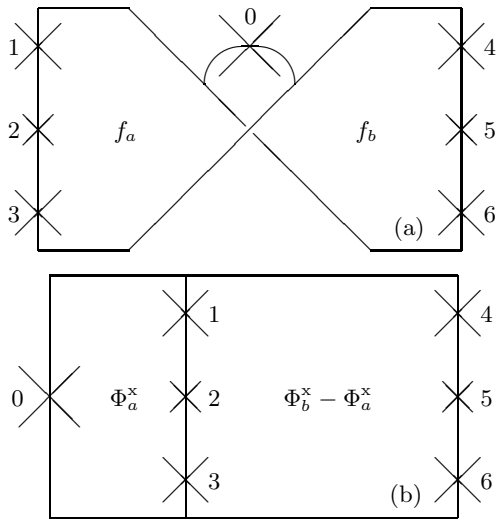


FIG. 5: Two 3JJ qubits with ferromagnetic Josephson coupling. (a): Twisted design. (b): Overlapping design.

Other variations are presented in Fig. 5. In Fig. 5(a), the relative twist between the qubit loops interchanges the role of the AF and FM configurations, so that the latter have the lowest energy. In particular, the strength of the direct FM Josephson coupling can overcome any residual AF inductive interaction. Junction 0 can presumably be fabricated between the crossing lines in the centre. In Fig. 5(b), one qubit loop is 01230 and the other is 04560; by choosing 1:2 area ratios, both qubits can be brought close to degeneracy with a homogeneous field, for $\Phi_a^x = \frac{1}{3}\Phi_b^x = \frac{1}{2}\Phi_0$. One obtains FM coupling without a twisted layout, but with strongly asymmetric qubits. The two discussed modifications can be combined: by current-biasing the junctions 0 in Fig. 5, one obtains tunable FM coupling.

In conclusion, we have demonstrated direct antiferromagnetic Josephson coupling between two individually controllable three-junction flux qubits. The coupling strength can be on the order of a Kelvin. We also proposed design modifications allowing tunable and/or ferromagnetic coupling. Future experimental work should also consider linear qubit arrays, to which the design of Fig. 1 is readily generalized.⁷

EI thanks the EU for support through the RSFQubit project. SvdP thanks the ESF pi-shift programme for a grant. MG acknowledges support by Grant No. VEGA 1/2011/05. AMB and AZ thank M.H.S. Amin, A.Yu. Smirnov, and M.F.H. Steininger for fruitful discussions.

* Electronic address: ilichev@ipht-jena.de

† Electronic address: alec@dwavesys.com

‡ Currently at UBC; email: zagoskin@physics.ubc.ca

¹ J.R. Friedman, V. Patel, W. Chen, S.K. Tolpygo, and J.E. Lukens, *Nature* **406**, 43 (2000); C.H. van der Wal, A.C.J. ter Haar, F.K. Wilhelm, R.N. Schouten, C.J.P.M. Harmans, T.P. Orlando, S. Lloyd, and J.E. Mooij, *Science* **290**, 773 (2000).

² J.E. Mooij, T.P. Orlando, L. Levitov, L. Tian, C.H. van der Wal, and S. Lloyd, *Science* **285**, 1036 (1999).

³ I. Chiorescu, Y. Nakamura, C.J.P.M. Harmans, and J.E. Mooij, *Science* **299**, 1869 (2003).

⁴ E. Il'ichev, N. Oukhanski, A. Izmalkov, Th. Wagner, M. Grajcar, H.-G. Meyer, A.Yu. Smirnov, A. Maassen van den Brink, M.H.S. Amin, and A.M. Zagoskin, *Phys. Rev. Lett.* **91**, 097906 (2003).

⁵ P. Bertet, I. Chiorescu, G. Burkard, K. Semba, C.J.P.M. Harmans, D.P. DiVincenzo, and J.E. Mooij, *cond-mat/0412485*.

⁶ L.S. Levitov, T.P. Orlando, J.B. Majer, and J.E. Mooij, *cond-mat/0108266*.

⁷ J.R. Butcher, graduation thesis (Delft University of Technology, 2002).

⁸ By considering “black box” devices in the outer arms, $U_J = U_a(2\pi(\frac{1}{2}+f_a)-\phi_0) + U_b(2\pi(\frac{1}{2}+f_b)+\phi_0) - E_0 \cos \phi_0$, one

readily verifies that the latter result also holds if the two qubits are asymmetric, biased, or of a different type.

⁹ Indeed, the remarks below (3) show the derivation to be analogous to the inductive case; cf. A. Maassen van den Brink, *Phys. Rev. B* **71**, 064503 (2005).

¹⁰ J.B. Majer, F.G. Paauw, A.C.J. ter Haar, C.J.P.M. Harmans, and J.E. Mooij, *Phys. Rev. Lett.* **94**, 090501 (2005).

¹¹ M. Grajcar *et al.*, *Phys. Rev. B* **69**, 060501(R) (2004).

¹² A. Izmalkov, M. Grajcar, E. Il'ichev, Th. Wagner, H.-G. Meyer, A.Yu. Smirnov, M.H.S. Amin, A. Maassen van den Brink, and A.M. Zagoskin, *Phys. Rev. Lett.* **93**, 037003 (2004).

¹³ Properly, χ' is the real part, effective at ω_T .

¹⁴ Ya.S. Greenberg, A. Izmalkov, M. Grajcar, E. Il'ichev, W. Krech, H.-G. Meyer, M.H.S. Amin, and A. Maassen van den Brink, *Phys. Rev. B* **66**, 214525 (2002).

¹⁵ A.Yu. Smirnov, *cond-mat/0312635*.

¹⁶ E.g., J. Lantz, M. Wallquist, V.S. Shumeiko, and G. Wendin, *Phys. Rev. B* **70**, 140507 (2004).

¹⁷ B.L.T. Plourde, J. Zhang, K.B. Whaley, F.K. Wilhelm, T.L. Robertson, T. Hime, S. Linzen, P.A. Reichardt, C.-E. Wu, and J. Clarke, *Phys. Rev. B* **70**, 140501(R) (2004); A. Maassen van den Brink and A.J. Berkley, *cond-mat/0501148*.